phys. stat. sol. (a) **97**, 87 (1986)

Subject classification: 61.70; 61.14; 61.16; S7

University of Antwerp (RUCA)[1]

The "Devil's Staircase" in CdP_2 and ZnP_2

By

C. MANOLIKAS[2], J. VAN TENDELOO, and S. AMELINCKX[3]

The defect structures occurring in the different phases of CdP_2 and ZnP_2 are studied by means of electron diffraction and high resolution electron microscopy. The occurrence of numerous planar interfaces in the β-phase of CdP_2 suggests a possible explanation for the series of microphases observed in this type of compound. The absence of thermal dilatation in certain small temperature ranges is explained by assuming that the thermal expansion is in fact compensated in such temperature intervals by the formation of new microphases with a different stacking resulting in smaller lattice parameters.

Die in den verschiedenen Phasen von CdP_2 und ZnP_2 auftretenden Strukturdefekte werden mittels Elektronenbeugung und hochauflösender Elektronenmikroskopie untersucht. Die Existenz von zahlreichen ebenen Grenzflächen in der β-Phase von CdP_2 legt eine mögliche Erklärung für die Serie von Mikrophasen, die in diesem Verbindungstyp beobachtet wird, nahe. Das Fehlen der thermischen Ausdehnung in gewissen kleinen Temperaturbereichen wird durch die Tatsache erklärt, daß sich in diesen Temperaturintervallen neue Mikrophasen mit unterschiedlicher Stapelung bilden, wodurch sich ein kleinerer Gitterparameter ergibt.

1. Introduction

The intriguing sequences of phase transitions observed in CdP_2 and in ZnP_2 have been discussed in a number of papers [1 to 7]. The crystallographic features of the high-temperature tetragonal β-form and of the low-temperature orthorhombic α-form of CdP_2 are summarized in Table 1 according to the literature.

It was shown that the tetragonal β-phase of CdP_2 undergoes a series of phase transitions in the temperature range from 100 to 400 K [5]. This was deduced mainly from the dependence of the lattice parameters a and c on temperature. The lattice parameters increase as a function of temperature, however, they remain constant in small temperature intervals (± 20 K wide) and change more rapidly in the temperature ranges adjacent to these small "plateaus", suggesting the occurrence of phase transitions around these temperatures. Macroscopic measurements of the thermal expansion reveal plateaus in the same temperature ranges [4]. The transformation process must obviously be such as to compensate for the normal thermal expansion in the temperature range of the plateau, where the effective thermal expansion coefficient thus becomes zero.

The plateaus occur in a slightly different temperature range on cooling and heating cycles, i.e. there is some thermal hysteresis. In the homologous α-ZnP_2 the structures corresponding with temperatures in the ranges between plateaus were assumed to be possibly incommensurately modulated and the series of phase transitions was considered to be an example of a "devil's staircase" [7]. It was further found by X-ray

---

[1] Groenenborgerlaan 171, 2020 Antwerp, Belgium.

[2] Permanent address: University of Thessaloniki, Thessaloniki, Greece.

[3] Also at: SCK/CEN, B2400-Mol, Belgium.

diffraction that the modulation period, as deduced from the positions of satellite reflections of high-order spots, changes only within the plateaus, decreasing with increasing temperature, and remains constant between steps; it is of the order of 20 nm [7]. However a detailed model for the phase transitions and in particular for the absence of thermal expansion in certain temperature ranges was not proposed as yet.

2. Structural Considerations

In the crystal structure all atoms are tetrahedrally coordinated, each cadmium atom being bonded to four phosphorus atoms, while each phosphorus atom is bonded to two cadmium atoms and two phosphorus atoms. The structure can be described as

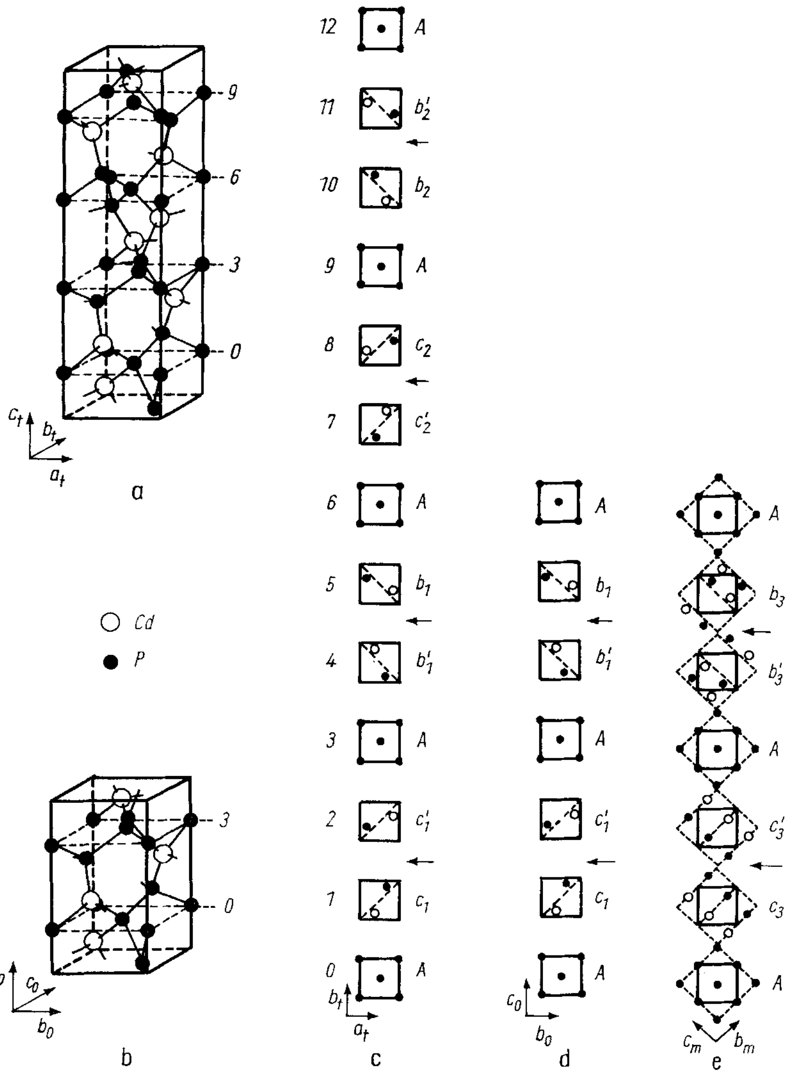

Fig. 1. Schematic representation of the CdP_2 and ZnP_2 structures: a) tetragonal β-CdP_2 structure (or α-ZnP_2), b) orthorhombic α-CdP_2 structure, c), d), e) key to describe mixed stacking sequences in β-CdP_2 (or α-ZnP_2), α-CdP_2, and monoclinic β-ZnP_2, respectively

Table 1

phase	space group	lattice parameters (nm)	ref.
β-CdP_2	tetragonal $P4_12_12$	$a = 0.529$ $c = 1.974$	[8]
	$P4_32_12$	$a = 0.528$ $c = 1.970$	[9]
α-CdP_2	orthorhombic $Pna2_1$ or Pnam	$a = 0.99 \pm 0.001$ $b = 0.5408 \pm 0.0005$ $c = 0.5171 \pm 0.0005$	[10]
α-ZnP_2	tetragonal $P4_32_12$	$a = 0.508 \pm 0.001$ $c = 1.859 \pm 0.005$	[11]
	$P4_12_12$	$a = 0.507$ $c = 1.865$	[9]
β-ZnP_2	monoclinic $P2_1/c$	$a = 0.88668(4)$ $b = 0.72913(5)$ $c = 0.75615(6)$ $\beta = 102.308(5)°$	[12]

being "layer-like" consisting of triplets of atom layers (Cd–P)–P–(Cd–P) parallel with the c-plane of the β-phase, which corresponds with the a-plane of the α-phase.

The bond lengths within a triplet are significantly shorter than those bridging different triplets. These triplet layers can be stacked in four different ways which occur in succession in the β-polymorph (Fig. 1 b).

The lattice parameter a_β of the tetragonal phase is very nearly equal to the geometrical mean of b_α and c_α of the orthorhombic α-phase, i.e. $a_\beta \approx \sqrt{b_\alpha c_\alpha}$ and moreover the c_β-parameter is approximately twice a_α, i.e. $c_\beta = 2a_\alpha$ (Table 1). The volume of the unit cell of the β-phase is twice that of the α-phase, i.e. $V_\beta \approx 2V_\alpha$ suggesting a close relationship between the α- and β-structures.

Idealizing the structure somewhat the β-phase can be represented by means of a stacking symbol for which the key is represented in Fig. 1 c,

β-phase: (b′Ac) (c′Ab′) (bAc′) (cAb) ... ,

where the brackets emphasize the triplet layers. The capital letter represents a pure phosphorus layer, whereas the small letters represent mixed layers of P–Cd consisting of a Cd atom surrounded by four P atoms and vice versa. b and c layers differ in the orientation of the diagonal, whereas dashed and undashed positions refer to interchanged positions for P and Cd (or Zn). The dashed and undashed positions are to a good approximation related by a translation 1/2[110] or 1/2[$1\bar{1}0$] (Fig. 1 c) which are symmetry translations for the A-layer.

The α-phase is orthorhombic; to the same approximation and using the same convention its structure can be represented by the stacking symbol (Fig. 1 d)

α-phase: (bAc) (c′Ab′) .

If we want to express the enantiomorphic nature of the structure by means of the notation introduced above we have to extend this somewhat. We note that the atoms in mixed layers (represented by small letters) are not arranged exactly along the diagonals of the squares in Fig. 1 but slightly left and right of these diagonals. We have therefore to distinguish the arrangements c_1 (and c_1') and c_2 (and c_2') as well as b_1 (and b_1') and b_2 (and b_2') where the lower index refers to the sense of the deviation from the diagonal arrangement.

If the right-handed structure $\beta(R)$ pictured layer by layer in Fig. 1, is represented by the stacking symbol

$$\dots (c_1'Ab_1')\ (b_1Ac_2')\ (c_2Ab_2)\ (b_2'Ac_1) \dots \beta(R)\,,$$

the left-handed $\beta(L)$ structure is represented by the symbol

$$\dots (c_1Ab_2')\ (b_2Ac_2)\ (c_2'Ab_1)\ (b_1'Ac_1') \dots \beta(L)$$

and the inversion related structure of $\beta^{(R)}$ by

$$\dots (c_2Ab_1)\ (b_1'Ac_1')\ (c_1Ab_2')\ (b_2Ac_2) \dots \beta(R, I)\,.$$

The empirical rules associated with the stacking symbol require that a triplet should start with the same letter by which the previous triplet ended; one of these should be dashed, the other undashed; furthermore the lower index should also be the same. The lower index can, but need not, be different for mixed layers on both sides of a pure phosphorus layer. The application of these rules leads for instance to the conclusion that a *periodic* stacking with a period containing an odd number of triplet layers is impossible.

A sixfold layer block which could occur periodically is for instance

$$(b'Ac)\ (c'Ab')\ (bAc')\ (cAb)\ (b'Ac')\ (cAb) \dots$$

which consists in fact of the juxtaposition of a β- and an α-like lamellae.

The presence of a singular sixfold lamella within a crystal of the β-phase is equivalent to the presence of a planar fault with a displacement vector $1/2[111]_\beta$ or $1/2[001]_\beta$.

The β-phase can be generated by introducing periodic faults separated by two triplets within the α-phase. In principle the α- and β-phases can in a crystal of a given hand transform one into the other for instance by slip along the $(001)_\beta$ plane, i.e. along the planes parallel with the triplet layers, the slip being performed by the propagation of partial dislocations producing a fault in their wake. Since in the actual structure the layers are very much "corrugated" it is unlikely that interpolytypic transformations will proceed by pure slip; thermal activation and short-range atom diffusion will be required to perform such a transformation. The high mobility of the metal atoms in these compounds, which are superionic conductors, makes this process relatively easy.

It is clear from Table 1 that the a-parameter of the monoclinic phase β-ZnP$_2$ is close to half the c-parameter of the tetragonal phase α-ZnP$_2$, whereas the b- and c-parameters of the monoclinic phase are both approximately equal to $\sqrt{2}$ times the a-parameter of the tetragonal phase. In fact, the monoclinic phase of ZnP$_2$ is rather closely related to the α-phase of CdP$_2$ and to the tetragonal phase. The atom positions as projected on the layer plane are represented schematically in Fig. 1 d, c in such a way as to emphasize the similarity with the other structures.

3. Observations. Electron Diffraction and Electron Microscopy

In an attempt to elucidate the mechanism of these phase transitions we have studied specimens of CdP$_2$ by means of electron diffraction and high resolution electron microscopy.

The material was prepared by the direct reaction between the constituents in evacuated quartz tubes, which yielded dark reddish crystals.

The high resolution observations as well as the electron diffraction patterns were made at room temperature after various heat treatments.

It was found that the material contained at least two different basic polymorphs or polytypes. The room temperature diffraction patterns of these different polymorphs are represented in Fig. 2; they may occur in different parts of the same crystal. Fig. 2a shows the $[010]_\alpha$ zone of the orthorhombic α-phase, whereas Fig. 2b and c refer to the $[001]_\alpha$ and $[100]_\alpha$ zones, respectively, of the same phase. Fig. 2c refers to the $[010]_\beta$ zone of the tetragonal β-phase. The corresponding high resolution images are reproduced in Fig. 3 a, b, and c, where also the unit cell projections are outlined.

The phase transitions in the tetragonal β-phase polymorph of CdP_2 have been the subject of the most detailed studies [1, 4, 5], for this reason we also focussed our ob-

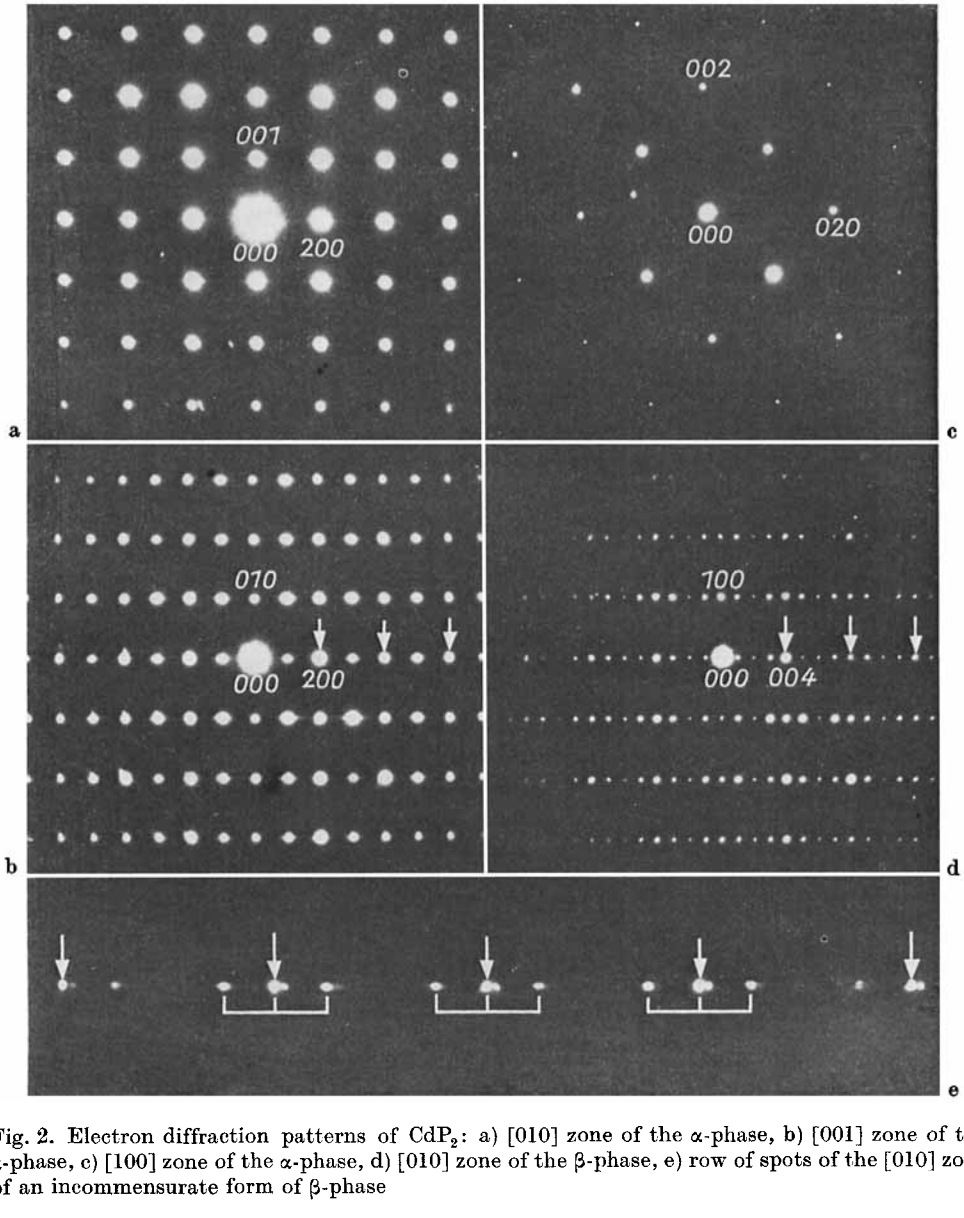

Fig. 2. Electron diffraction patterns of CdP_2: a) [010] zone of the α-phase, b) [001] zone of the α-phase, c) [100] zone of the α-phase, d) [010] zone of the β-phase, e) row of spots of the [010] zone of an incommensurate form of β-phase

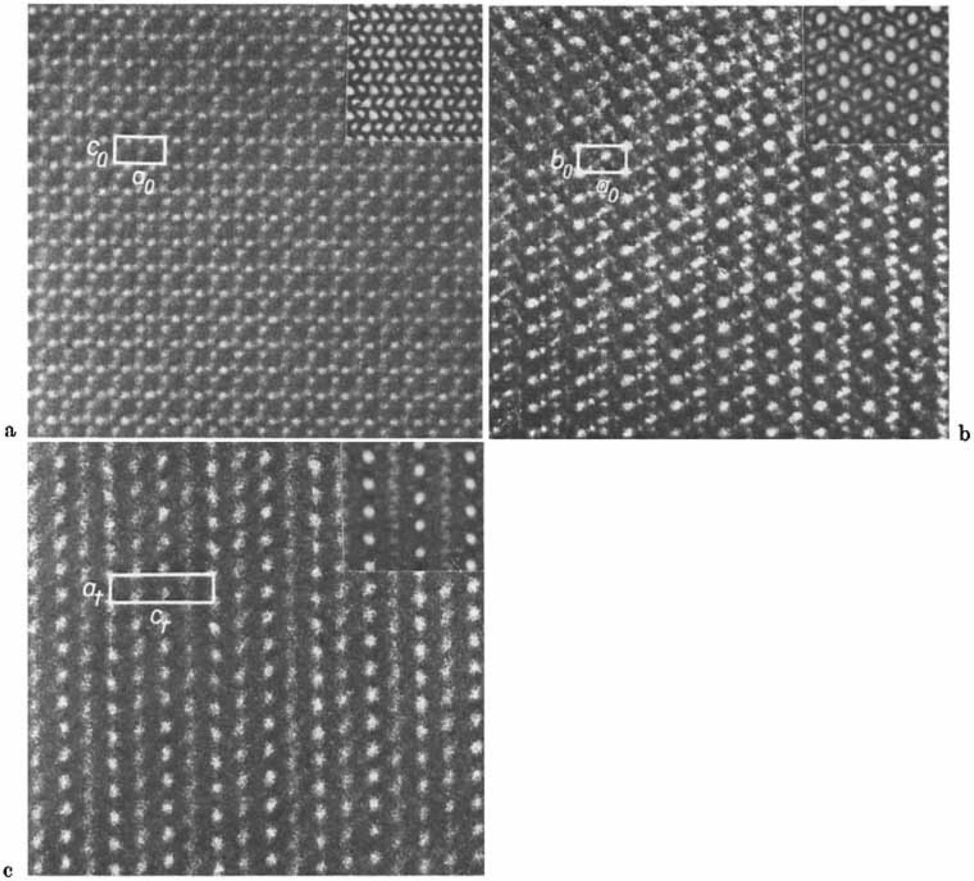

Fig. 3. High resolution images of CdP_2 (cfr. Fig. 2): a) [010] zone of the α-phase, b) [001] zone of the α-phase, c) [010] zone of the β-phase. The insets are computed images

servations on this polymorph. It is found by high resolution electron microscopy that the local period is not always strictly defined; in a number of parts of the crystal one finds a mixture of spacings such as 4 and 6 (Fig. 4b) or occasionally 4 and a singular layer of 5 (Fig. 4a). Usually rather heavily disordered sequences are observed (Fig. 5).

In the diffraction pattern corresponding with a large area containing faults such as shown in Fig. 5 the spots corresponding with the l = even reflections remain sharp, but the spots with l = odd acquire weak, poorly resolved satellite spots (Fig. 6). This suggests that the six- as well as the four-layer periodicity result from two-layer α-lamellae stacked differently. In a number of cases, in CdP_2 as well as in ZnP_2 the diffraction pattern is slightly incommensurate, as shown in Fig. 2, which is one row of spots of a pattern similar to Fig. 2d. The diffraction pattern can be considered as consisting of the most intense "basic" spots, indicated by arrows in Fig. 2e and pairs of satellites associated with these basic spots. The satellites are separated from the basic spots by a distance which is $\frac{1}{4} - \varepsilon$ times the distance between basic spots. The structure corresponding with these basic spots would have a lattice parameter, in the direction normal to the layers, equal to the thickness of one triplet layer (bAc).

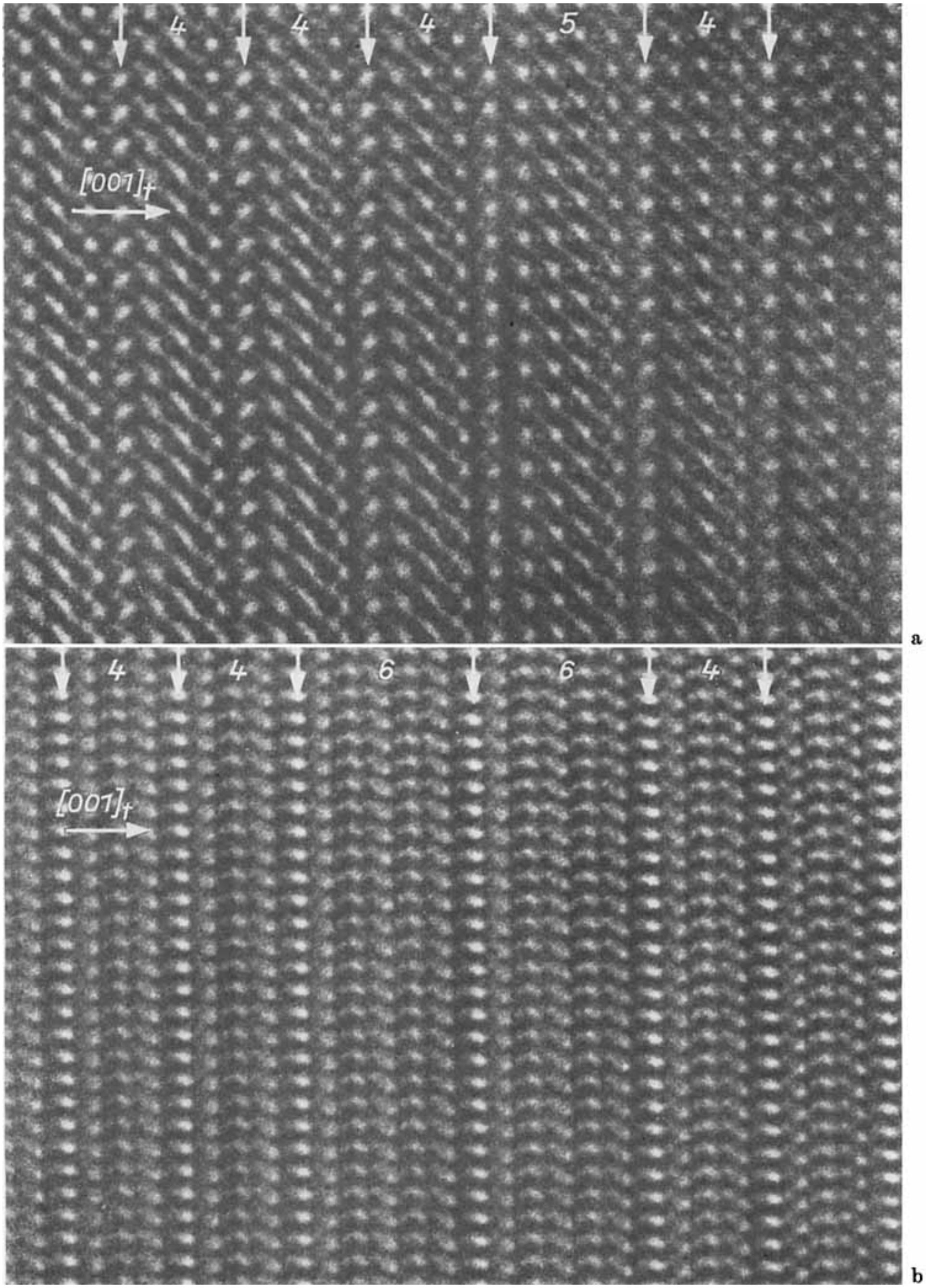

Fig. 4. High resolution images of faulted sequences in the β-phase of CdP_2 along the [110]β zone: a) sequence of fourfold lamella containing a singular fivefold lamella, b) mixture of fourfold and sixfold lamellae

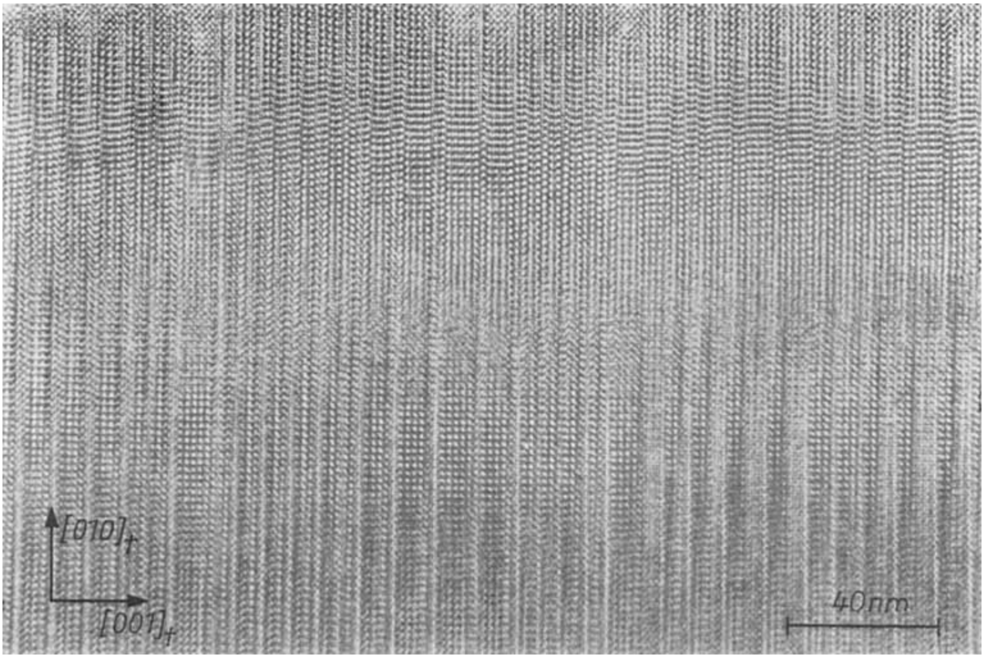

Fig. 5. High resolution image of faulted crystal part of the β-phase of CdP_2 along the $[100]_\beta$ zone

The average period as deduced from the "satellite" separation is slightly larger than c_β. This is consistent with a mixing of spacing, e.g. 4 and 6. Also the optical diffraction patterns of different parts of the photographic negative of a high resolution image such as Fig. 5 reveal a_α and $2a_\alpha \approx c_\beta$ stacking periods and moreover exhibit incommensurate spots (Fig. 7) due to the presence of a long-period modulation.

The results obtained by X-ray diffractometry show that in ZnP_2 the long modulation period changes in the temperature range corresponding with the plateaus [7]. We suggest that this also happens in CdP_2, i.e. that the layer arrangement changes by the propagation of planar interfaces in the temperature ranges corresponding with the plateaus. The changes must be such that with increasing temperature a larger proportion of β-type arrangements are formed since this makes the c_β-parameter shrink. Between plateaus the arrangements do not change and therefore the modulation period remains the same, but thermal expansion is observed.

Under the appropriate diffraction conditions the crystals of β-CdP_2 and of tetragonal α-ZnP_2 exhibit bands of different shade (Fig. 8), strictly limited by c-planes. The presence of these bands does not seem to affect the diffraction pattern; in particular there is no spot splitting, showing that the structures within the bands of different shade are based on a common lattice. Since the structure is non-centrosymmetric (point group 422) and enantiomorphic, the bands might correspond either to the left- and right-handed crystal parts or to crystal parts related by an inversion operation.

Such bands are not visible in bright field images whatever be the diffraction conditions; only the limiting interfaces may be imaged. In the symmetrical orientation, i.e. exactly along a $[100]_\beta$ zone there is no contrast neither in the bright field image, nor in the dark field image. However, if the crystal is tilted so as to excite higher-order

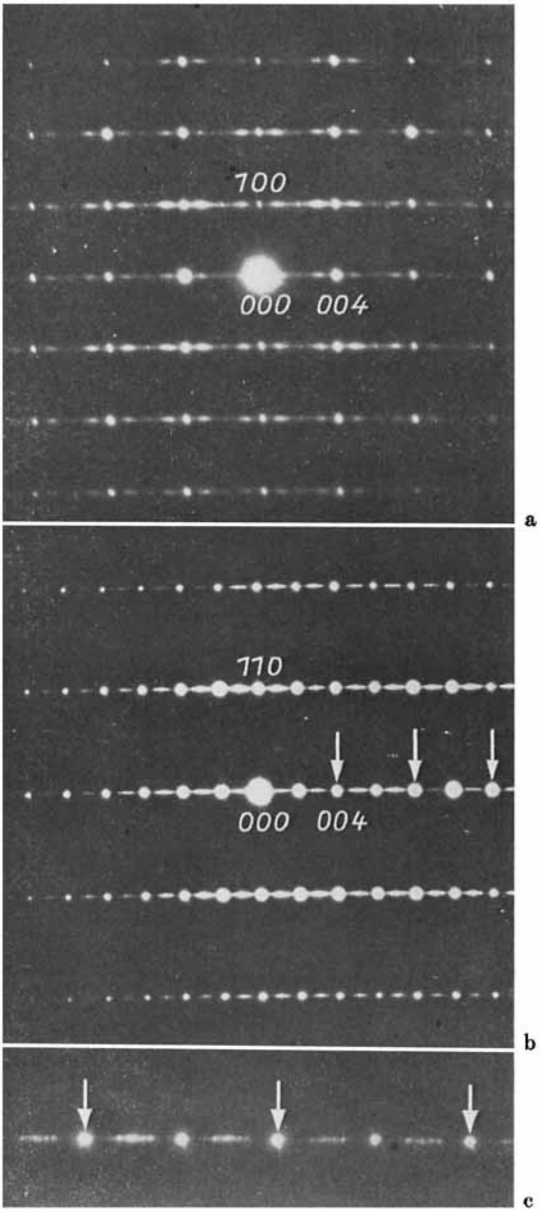

Fig. 6. Electron diffraction pattern of a disordered β-phase crystal of CdP_2: a) $[010]_\beta$ zone pattern, b) $[1\bar{1}0]_\beta$ zone pattern: note that the l = even spots remain sharp whereas the l = odd spots have acquired satellites, c) Magnified image of one row of spots of b)

Laue zones, and dark field images are made in pairs of such spots, bands appear in a strong bright–dark domain contrast superimposed on the lattice fringes. These contrast features suggest strongly that the bands correspond with inversion domains, the contrast being due to the violation of Friedel's law [13]. The absence of contrast in the exact $[100]_\beta$ zone, which is parallel with a twofold axis, is then due to the fact that the projected structure along this zone presents a centre of symmetry. The absence of domain contrast in the bright field image for all orientations seems to exclude that the bands should be enantiomorphic twins.

This conclusion is based on the following reasoning: Let the structure amplitude of the right-handed crystal be

$$F^{\mathrm{R}}_{hkl} = \sum_i f_i \exp\left[2\pi i(hx_i + ky_i + lz_i)\right].$$

The left-handed structure can be obtained for instance by applying a mirror operation with respect to a plane, e.g. the (100) plane. The structure factor of the left-handed crystal with respect to the same reference frame is then

$$F^{\mathrm{L}}_{hkl} = \sum_i f_i \exp\left[2\pi i(-hx_i + ky_i + lz_i)\right] = F^{\mathrm{R}}_{\bar{h}kl}.$$

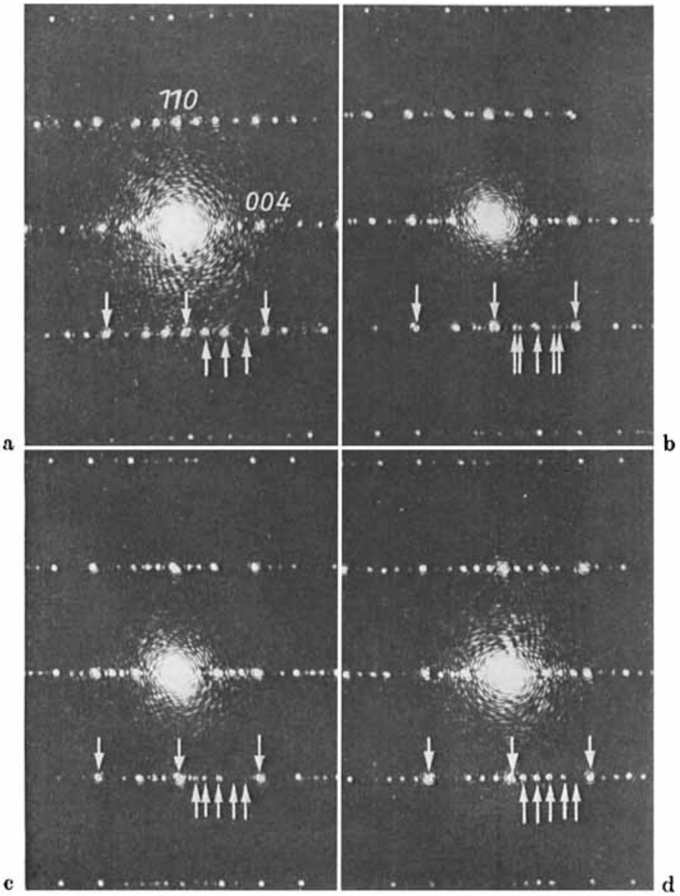

Fig. 7. Optical diffraction patterns of different parts of a high resolution image taken along $[110]_\beta$: a) β-phase: fourfold lamellae, b) and c): mixtures of fourfold and sixfold lamellae producing incommensurate spots, d) sixfold superperiod

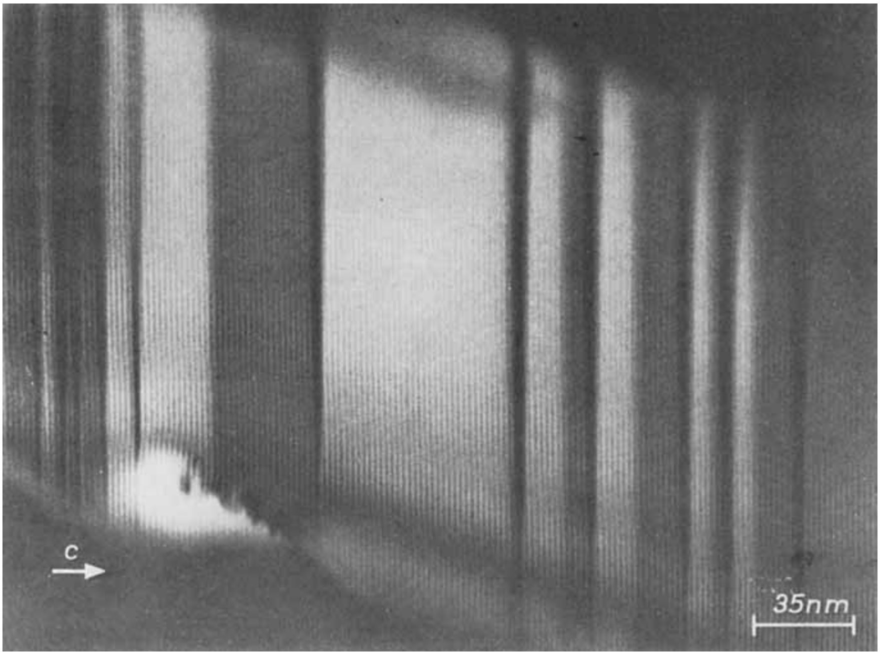

Fig. 8. Dark field image of α-ZnP_2 made in a pair of spots belonging to a high-order Laue zone The bounds of different shade superimposed in the lattice fringes 1.9 nm are inversion domain.

Since the structure does not contain a mirror plane we have in general $F^{R}_{\bar{h}kl} \neq F^{R}_{hkl}$ and therefore also in general $F^{R}_{hkl} \neq F^{L}_{hkl}$; structure amplitude contrast should thus be observed in bright and dark field images for adequately chosen reflections. The same applies mutatis mutandis for mirror operations with respect to planes such as (010) or (001). No such contrast is observed.

The structure factor of the structure related by an inversion operation to the original one is given by

$$F^{IR}_{hkl} = \sum_i f_i \exp\,[2\pi i(-hx_i - ky_i - lz_i)] = F^{R}_{\bar{h}\bar{k}\bar{l}}\,.$$

By Friedel's law $|F_{hkl}| = |F_{\bar{h}\bar{k}\bar{l}}|$ and therefore in general no structure amplitude contrast is possible; however, contrast based on the violation of Friedel's law is possible in the dark field images made in multiple beam situations [13].

One might further argue that the bands correspond with different phases, for instance α and β, for which the diffraction spots are partly coincident. However, in this case one should have observed contrast in the bright field image at least for certain orientations. Moreover the lattice fringe spacing would have been different in two successive bands, which is not the case. We conclude that the only possible model, in accord with all observations, consists in considering the bands as inversion domains.

In the monoclinic phase β-ZnP_2 a different type of planar defect based on the stacking of the same type of layers becomes possible. Since the layer plane is no longer a symmetry plane of the lattice, twinning on this plane becomes possible. This is shown in Fig. 9. The diffraction pattern across a twin interface is shown in Fig. 9c. Corresponding [011] directions are indicated in the two components of the twin.

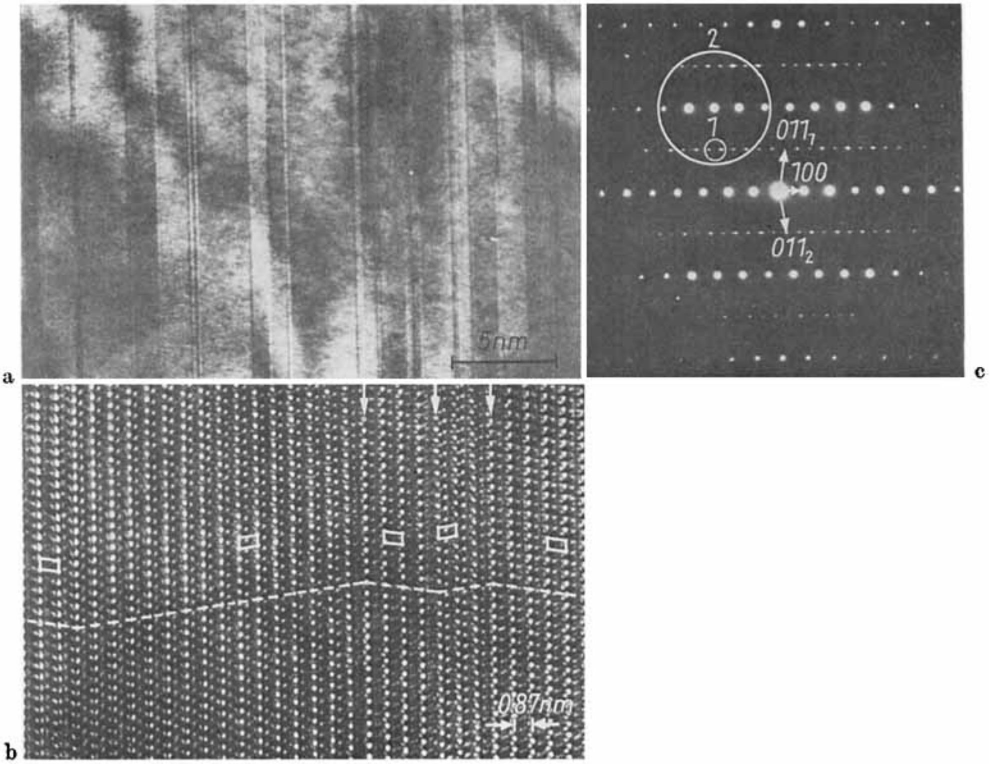

Fig. 9. Twinning on the (100) plane of monoclinic β-ZnP_2: a) dark field image made in the spots surrounded by the small circle 1 of Fig. 9c; b) dark field high resolution image made in the spots surrounded by the large circle 2 of Fig. 9c

A dark field image made in a pair of twin-related spots, such as those surrounded by the small circle 1, is reproduced in Fig. 9a. The twin exhibits weak domain contrast and also the twin boundaries are imaged as fine lines. Since the two spots originate from different parts of the twin no lattice fringes corresponding to the spot separation are produced. Dark field images made in a single one of these spots produce a strong dark-bright diffraction contrast of twin bands. It also reveals ending microtwin lamella, some of which are terminated at both ends in the crystal.

In the diffraction pattern the spots with $l = 2n$ remain sharp, since they belong to the reciprocal lattice of both parts of the twin, whereas the spots with $l = 2n + 1$ become somewhat elongated as a result of the variations in width of the microtwin lamella.

The high resolution image of Fig. 9b clearly demonstrates the presence of microtwins bounded by planes parallel with the layer planes. The details of the image, i.e. the geometry of the weak dots suggest that the interfaces are presumably not twins of the structure, only of the lattice.

4. Discussion

The mixing of spacings in a "regular" fashion is known to give rise in the diffraction pattern to sharp peaks at positions corresponding with the average spacing, which can be pseudo-incommensurate (fractional) or incommensurate within the experimental error [14].

The small plateaus in the thermal expansion, deduced from the lattice parameter changes as well as from macroscopic dimensional changes, could possibly be attributed to changes in the stacking sequence taking place at the phase transition resulting in a decrease of the average interlayer spacing largely compensating the thermal expansion. This could be achieved by mixing α- and β-strips, the concentration of β-strips increasing stepwise in the small temperature ranges, where the thermal expansion is found to be zero. However, such a process would affect the lattice parameter but not necessarily the macroscopic dimensions, unless the triplet lamella in the β-arrangement would be "thinner" than those in the α-arrangement. The high resolution images are not sensitive enough to give evidence in this sense.

Taken at their face value the X-ray results (Table 1) show that the triplet layers in the α-phase are on the average slightly "thicker" than those in the β-phase, the difference in thickness being 2.5×10^{-3} nm per layer. An increase in the proportion of layers in a β-arrangement as compared to those in the α-arrangement would thus lead to a decrease in the dimensions along the *c*-direction.

From the measured thermal expansion coefficient ($\alpha = 4.8 \times 10^{-6}\,K^{-1}$) we can deduce that the thermal expansion over a temperature range of about 20 K as is observed, can be compensated by a change of one α-arrangement into a β-configuration about every twentieth triplet layer, which is a reasonable figure.

It was found that the *a*-parameter exhibits "plateaus" in the same temperature intervals as the *c*-parameter. An increase in the proportion of lamella in the β-arrangement would thus have to lead to a decrease of the *a*-parameter as well, which is possible since also the *a*- and *b*-parameters of the α-phase are different from those of the β-phase.

A possible model for the sequence of transitions in the β-phase could thus be as follows. At the lower end of the temperature range the crystal contains a certain proportion of layers in the low-temperature α-configuration. If these α-lamella equally adopt four possible orientations, either with their *b*- or *c*-axis parallel or antiparallel with the same *a*-axis of the β-phase and with their long-period axis parallel in both polymorphs α and β, i.e. with their layer planes parallel, the resulting crystal still exhibits overall tetragonal symmetry. With increasing temperature the proportion of α-arrangement may decrease stepwise in well-defined temperature intervals. This would lead to a decrease of the macroscopic dimension as well as of the measured c_β-spacing, which should of course be distinguished from the long period of the modulated structure. A number of different quasi-periodic arrangements, possibly with long periods, comprising α- and β-type lamella in varying proportions would exist between two successive plateaus. The changes in arrangement would occur in the small temperature ranges where the effective thermal expansion is zero. Between plateaus thermal expansion of a solid with a well-defined layer arrangement (i.e. polytype) would occur.

The fault vector associated with the presence of a singular sixfold lamella is of the type 1/2[111] or 1/2[001]. The diffraction pattern of a β-phase crystal containing a disordered sequence of such faults will therefore exhibit sharp reflections $\boldsymbol{H}$ for $\boldsymbol{H} \cdot \boldsymbol{R} = 0$ (mod. 1) and streaked reflections for $\boldsymbol{H} \cdot \boldsymbol{R} \neq 0$ (mod. 1). This is indeed observed in the $[100]_\beta$ and $[110]_\beta$ zone pattern, where the spots with l = odd become streaked whilst the spots with l = even remain sharp (Fig. 6).

We have obtained direct visual evidence for the growth of planar defects on cooling a specimen of the β-phase to liquid nitrogen temperature in the microscope. Fig. 10

shows an array of planar interfaces in the [001] zone of β-CdP_2, as observed in the one-dimensional lattice fringes mode. This mode exhibits more clearly the singularities in the lattice spacing than does the high resolution image. The planar interfaces indicated by arrows have clearly extended either by the motion of the bordering partial dislocations or by the extension of a hair-pin-shaped loop [15]. The motion is slow but steady; it took of the order of 30 min to change from Fig. 9a into Fig. 9d. The motion is thus presumably not pure slip, but apparently requires short-range diffusion. The local fringe spacing has changed as expected from the proposed model.

The planar faults on the *c*-plane in the β-form are of a peculiar nature, they do not behave as usual stacking faults. They produce some singular lines in the pattern of 1.9 nm lattice fringes parallel with the fault planes. The lattice fringes on both sides

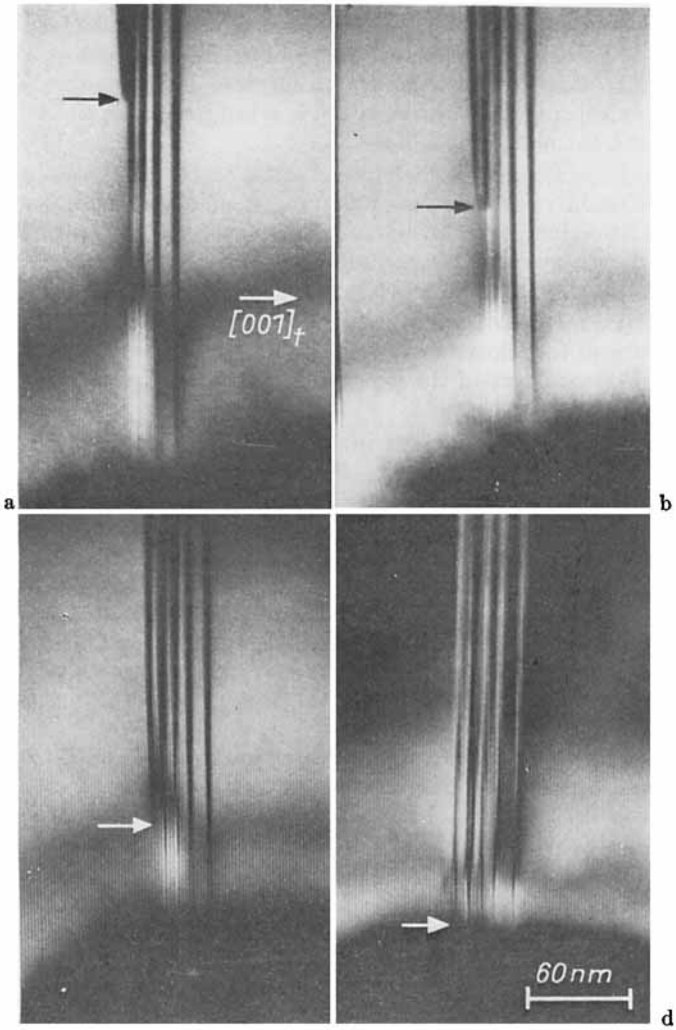

Fig. 10. Dark field lattice images of a sequence of faults taken at different times at ≈180 K. The faults indicated by arrows have extended during the observation period and reached the edge of the specimen

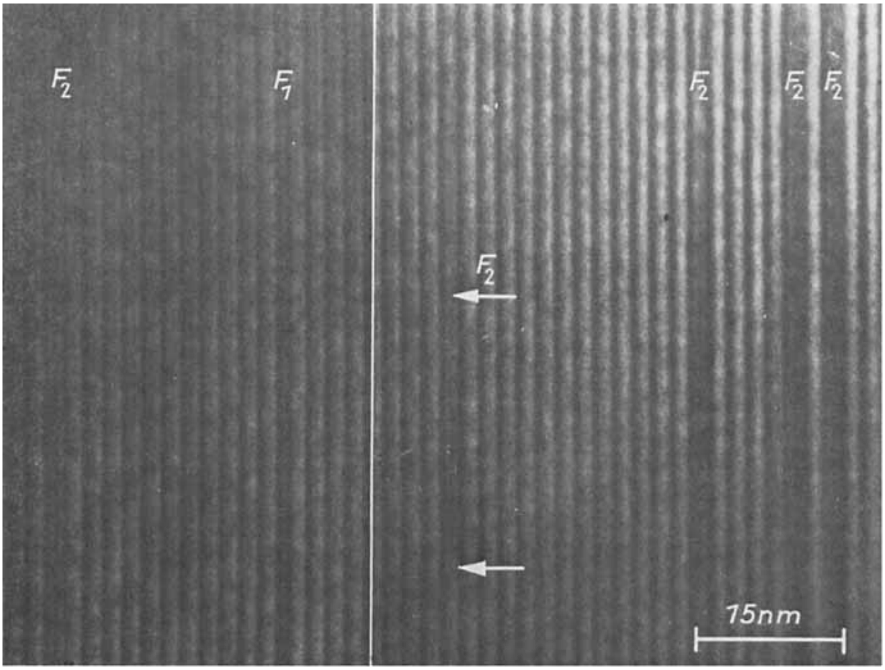

Fig. 11. Lattice fringes (1.9 nm) with β-phase of CdP_2. Note the singular fringes with shift (F_1) and without shift (F_2)

of the fault are nevertheless "in phase" in many cases. However, in a number of cases the fault may cause a shift of approximately 1/2 interfringe (Fig. 11). The crystal parts on both sides of the faults are thus not visibly displaced in many cases. This is confirmed by high resolution images.

Neither a dislocation configuration of fringes, nor dislocation contrast is observed where the faults terminate within the crystal. A possible origin of the contrast might be that cations are disordered along such layers. It is not obvious why this should be preferentially along such planes since the mobility of Zn or Cd ions is in fact much higher along the c-axis than perpendicular to it as deduced from measurements of the electrical conductivity [16].

Fig. 11 shows a detailed view using one-dimensional lattice fringes of a stacking configuration consisting of a mixture of fourfold and twofold lamella, observed at room temperature after having cooled the specimen. This type of mixture we believe is responsible for the different phases.

5. Conclusions

In summary we believe that the plateaus in the thermal expansion curves result from the fact that the proportion of α- and β-like layer arrangements changes rather rapidly in finite temperature ranges but remains constant outside of these. In such temperature ranges the transformation of a number of regularly spaced α-like arrangements into β-like arrangements causes the average lattice parameters and the dimensions of the specimen to decrease, compensating in this way for the normal thermal expansion. On heating the proportion of β-type arrangements (the high-temperature phase would increase whereas on lowering the temperature the reverse would take place. The incommensurate diffraction spots result from the mixture of long spacings comprising four and six layers (i.e. 4 + 2). The high resolution images demonstrate that such mixtures of stackings occur and the optical diffraction patterns of such images demonstrates the occurrence of modulated structures. Also electron diffraction patterns over a relatively large area reveal satellites corresponding with long modulation periods of the same order of magnitude as those observed in ZnP_2 [7], i.e. 15 to 20 nm.

Our observations do not allow to propose a detailed model for the stacking sequences present in the different phases, i.e. in the temperature ranges between the "plateaus", especially since no high resolution images could be obtained at low temperature, where most plateaus occur. By analogy with our observations at room temperature, after cooling and heating cycles, we believe that a possible model could be as follows. At the lowest temperature the structure is entirely α. The structure formed at a slightly higher temperature could for instance be of the type $\alpha_n\beta$ with n of the order of 20. The next structures formed on increasing the temperature could then for instance be $\alpha_{n-1}\beta$, $\alpha_{n-2}\beta$, $\alpha\beta$, $\alpha\beta_n$ until at high temperature the structure is entirely β. We suggest that this succession of microphases forms a devil's staircase [17].

The measured c_β parameter refers in fact to the average thickness of four layers. The superlattice spacing of the modulated structure refers to the quasi-period given by the average thickness of the lamella $\alpha_n\beta$ or $\alpha\beta_n$.

References

[1] N. N. Sirota, A. M. Antyrekhov, and E. M. Smolyarenko, Izv. Akad. Nauk. SSSR, Ser. neorg. Mater. **13**, 358 (1977).

[2] A. V. Sheleg, A. A. Kutas, and N. P. Tekhanovich, phys. stat. sol. (a) **58**, K179 (1980).

[3] A. V. Sheleg, E. Peljo, and P. Suortti, phys. stat. sol. (a) **63**, 751 (1981).

[4] A. V. Sheleg, V. P. Novikov, and L. K. Orlik, Soviet Phys. – Solid State **22**, 1444 (1980).

[5] A. V. Sheleg and V. P. Novikov, Soviet Phys. – Solid State **24**, 2000 (1982).

[6] A. V. Sheleg and V. V. Zaretskii, Soviet Phys. – Solid State **25**, 1830 (1983).

[7] A. V. Sheleg and A. V. Zaretskii, phys. stat. sol. (a) **86**, 517 (1984).

[8] E. Parthé, Crystal Chemistry and Tetrahedral Structures, Gordon & Breach, New York 1964 (p. 127).

[9] M. Stackelberg and P. Paulus, Z. phys. Chem. **28B**, 427 (1935).

[10] J. Goodyear and G. A. Steigmann, Acta cryst. **B25**, 2371 (1969).
O. Olofsson and J. Gullman, Acta cryst. **B26**, 1883 (1970).

[11] J. G. White, Acta cryst. **18**, 217 (1965).

[12] M. E. Fleet and T. A. Mowles, Acta cryst. **C40**, 1778 (1984).

[13] R. Serneels, M. Snykers, P. Delavignette, R. Gevers, and S. Amelinckx, phys. stat. sol. (b) **58**, 277 (1973).

[14] K. Fujiwara, J. Phys. Soc. Japan **12**, 7 (1957).

[15] J. Van Landuyt and S. Amelinckx, J. Solid State Chem. **6**, 222 (1973).

[16] V. P. Novikov, Dokl. Akad. Nauk BSSR **26**, 697 (1982).

[17] P. Bak, Rep. Progr. Phys. **45**, 587 (1982).

(Received July 4, 1986)